Analytical Assessment for Transient Stability Under Stochastic Continuous Disturbances

Ping Ju, *Senior Member, IEEE*, Hongyu Li, *Student Member, IEEE*, Chun Gan, *Member, IEEE*, Yong Liu, *Member, IEEE*, Yiping Yu, *Member, IEEE*, and Yilu Liu, *Fellow, IEEE*

***Abstract*—With the growing integration of renewable power generation, plug-in electric vehicles, and other sources of uncertainty, increasing stochastic continuous disturbances are brought to power systems. The impact of stochastic continuous disturbances on power system transient stability attracts significant attention. To address this problem, this paper proposes an analytical assessment method for transient stability of multimachine power systems under stochastic continuous disturbances. In the proposed method, a probability measure of transient stability is presented and analytically solved by stochastic averaging. Compared with the conventional method (Monte Carlo simulation), the proposed method is many orders of magnitude faster, which makes it very attractive in practice when many plans for transient stability must be compared or when transient stability must be analyzed quickly. Also, it is found that the evolution of system energy over time is almost a simple diffusion process by the proposed method, which explains the impact mechanism of stochastic continuous disturbances on transient stability in theory.**

***Index Terms*—Energy function method, stability probability, stochastic averaging method, stochastic continuous disturbances, stochastic differential equations (SDEs), transient stability.**

I. Introduction

POWER systems are operated under uncertainty and randomness, so there is an increased need for probabilistic transients stability assessment tools [1]. The basic theory of probabilistic transient stability assessment was established by Billinton and Kuruganty to handle stochastic fault type, fault location, fault clearing time and system operating conditions that can affect transient stability [2]. Much research has been conducted on this topic [3]–[8]. With the growing integration of renewable power generation [9]–[11] plug-in electric vehicles [12], [13], uncertain dynamic loads [14], and so on, stochastic continuous disturbances are increasing, which will bring new concerns for transient stability. It has been proven that the cumulative effects of stochastic continuous disturbances can cause system state trajectories to leave any bounded domain after a sufficiently long time, even though the same system can tolerate one severe fault at its equilibrium point [15]–[17]. Previous transient stability assessment methods have difficulties in handling stochastic continuous disturbances.

Stochastic differential equations (SDEs) are widely applied to model power systems under stochastic continuous disturbances [18]–[23]. In [24], a systematic method was proposed to model power systems under stochastic continuous disturbances as a set of stochastic differential algebraic equations. In [25], stochastic differential equations were adopted to describe continuous wind speed models.

Monte Carlo simulation is a powerful tool for analyzing SDEs. In [26], a novel framework of stochastic transient stability assessment was proposed with Monte Carlo simulation. In [27], the authors used the importance sampling method to improve the efficiency of Monte Carlo simulation. In [28], Monte Carlo simulation and the stochastic Lyapunov stability method were combined to assess power system transient stability under stochastic continuous disturbances. The Monte Carlo simulation has advantages on adaptability, but the computational burden often makes it undesirable. Moreover, the impact mechanism is not clear with Monte Carlo simulation [29].

To overcome the weakness of Monte Carlo simulation, analytical assessment methods based on stochastic theory have been developed. In [30], the evolution of state's probability density was solved by the Fokker-Planck's equation to determine the impact of stochastic load perturbations on system stability. In [31], voltage collapse of power systems under stochastic continuous disturbances was investigated. However, the above methods are applied in simple power systems and the applications in multimachine power systems were not addressed well.

Although transient stability assessment of power systems under stochastic continuous disturbances has been considered and partly solved in the last decades, there are still some deficiencies in existing methods: 1) the majority of assessment methods are based on Monte Carlo simulation, which suffers low computational efficiency and unclear impact mechanism; 2) the application of analytical assessment methods in multi-machine power systems encounters difficulties, due to their complexity; 3) probability measure of transient stability under stochastic continuous disturbances has not been proposed.

Manuscript received January 7, 2017; revised April 30, 2017; accepted June 11, 2017. Date of publication June 28, 2017; date of current version February 16, 2018. This work was supported by the National Basic Research Program of China (973 Program) (2013CB228204). Paper no. TPWRS-00022-2017. *(Corresponding author: Hongyu Li.)*

P. Ju, H. Li, and Y. Yu are with the College of Energy and Electrical Engineering, Hohai University, Nanjing 211100, China (e-mail: pju@hhu.edu.cn; hongyu.li.1990@gmail.com; yyiping@hhu.edu.cn).

C. Gan and Y. Liu are with the Department of Electrical Engineering and Computer Science, University of Tennessee, Knoxville, TN 37996 USA (e-mail: cgan@utk.edu; yliu66@utk.edu).

Y. Liu is with the Department of Electrical Engineering and Computer Science, University of Tennessee, Knoxville, TN 37996 USA, and also with the Oak Ridge National Laboratory, Oak Ridge, TN 37831 USA (e-mail: liu@utk.edu).

Color versions of one or more of the figures in this paper are available online at http://ieeexplore.ieee.org.

Digital Object Identifier 10.1109/TPWRS.2017.2720687

To address the deficiencies listed above, this paper proposes a novel analytical assessment method for multi-machine power systems under stochastic continuous disturbances. Stability probability, which is presented as a measure of transient stability under stochastic continuous disturbances, is analytically solved by the stochastic averaging. Moreover, comparisons with Monte Carlo simulation in the Kundur's 4-machine 2-area system and a 50-machine 145-bus test power system are given to verify the accuracy and efficiency of the proposed method. The proposed method has two significant advantages: First, the proposed method is computationally efficient. Second, the impact mechanism of stochastic continuous disturbances on transient stability is clear by the proposed method.

The organization is as follows: Section II introduces models of multi-machine power systems under stochastic continuous disturbances. Section III illustrates transient stability under stochastic continuous disturbances. Section IV presents the analytical assessment method for transient stability under stochastic continuous disturbances. Section V gives simulation examples and insights. Section VI offers a conclusion. Derivations are shown in the Appendix.

II. Models of Multi-Machine Power Systems Under Stochastic Continuous Disturbances

In this study, the classical model has been adopted initially. Then the stochastic model of multi-machine power systems under stochastic continuous disturbances can be expressed as a set of Itō SDEs [15], [16], [30]

$$\begin{cases} \dfrac{\mathrm{d}\delta_i}{\mathrm{d}t} = \omega_N \omega_i \\ M_i \dfrac{\mathrm{d}\omega_i}{\mathrm{d}t} = P_{mi} - G_{ii}{E_i}^2 - \sum_{j=1, j\neq i}^{n} P_{\max ij} \sin(\delta_i - \delta_j) \\ \quad -D_i\omega_i + \sigma_i W_i(t) \end{cases} \qquad i = 1, 2, \ldots, n \tag{1}$$

where $\sigma_i W_i(t)$ are stochastic continuous disturbances; $W_i(t)$ are standard Gaussian white noises; σ_i are disturbance intensities; $P_{\max ij} = E_i E_j B_{ij}$; δ_i, ω_i, M_i, P_{mi}, E_i, and D_i are rotor angle, rotor speed deviation, inertia coefficient, mechanical power, internal voltage, and damping coefficient of ith generator, respectively; G_{ii} is the ith diagonal element of conductance matrix; B_{ij} is the element in the ith row and jth column of susceptance matrix; and ω_N is the synchronous machine speed.

Because the network and load are merged, stochastic continuous disturbances $\sigma_i W_i(t)$ are added on machine equations [15], [16], [30]. Because stochastic continuous disturbances are from the mechanical power P_{mi} and the quadratic term of self-conductance $G_{ii}E_i^2$, they denote the stochastic unbalanced active power between the generation and load.

'Stochastic continuous disturbances' are referred to as 'stochastic excitation' in stochastic theory terminology [32]. Considering that 'excitation' is easily confused with the excitation of the magnetic field in electric motors, we prefer 'stochastic continuous disturbance' as the 'stochastic excitation' for clarity in this paper.

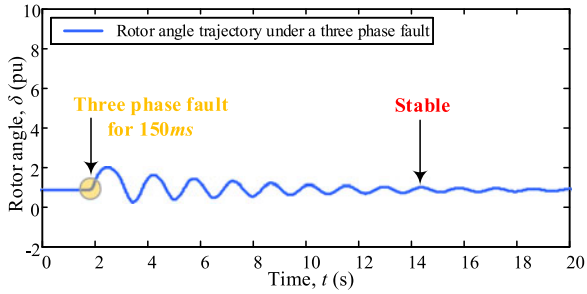

Fig. 1. Rotor angle trajectory of a power system under a three phase fault.

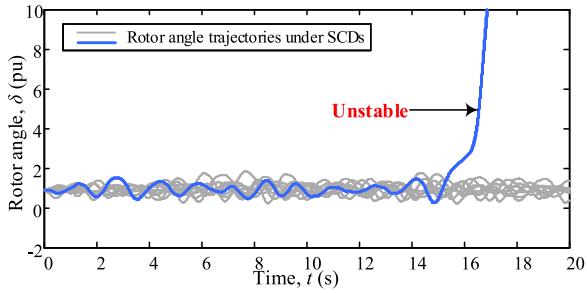

Fig. 2. Rotor angle trajectories of a power system under stochastic continuous disturbances.

III. Power System Transient Stability Under Stochastic Continuous Disturbances

A. Problems Faced With Transient Stability

It is known that contingencies can greatly impact power system transient stability, but power system transient stability also faces new problems with increasing stochastic continuous disturbances. It was proved that even if a dynamic system can tolerate one severe fault at its equilibrium point, cumulative effects of stochastic continuous disturbances can cause its state trajectories to leave any bounded domain after a sufficiently long time [15]–[17]. For instance, a single-machine infinite-bus power system is subjected to a three-phase fault on the transmission line for 150 *ms*, and its rotor angle trajectory is stable as shown in Fig. 1. However, when the same system is subjected to stochastic continuous disturbances, one of 10 trajectories exhibits unexpected behavior and becomes unstable as shown in Fig. 2. Therefore, transient stability assessment methods considering only system faults are incomplete, which will have difficulties in handling stochastic continuous disturbances.

B. Transient Stability Probability

The system is either stable or unstable at a certain time. However, when the stochastic continuous disturbances are introduced to a power system, one cannot answer whether the system is deterministically stable or unstable in the following time because the transient stability becomes a random event [30], [31]. The probability of states being within the stability region represents stability probability. From the view of operational decision-making, stability probability is a proper measure to evaluate the transient stability under stochastic continuous disturbances.

It is reasonable that the system with higher stability probability is more probabilistically stable. Stability probability can be expressed by the following form:

$$P\left(t|\boldsymbol{X}_0\right) = P\left\{\boldsymbol{X}\left(\tau\right) \in \Omega, \tau \in (0,t]|\boldsymbol{X}_0 \in \Omega\right\} \tag{2}$$

where $P(t\,|\,\boldsymbol{X}_0)$ is the probability of states being in stability region Ω, within the time interval $[0,\ t)$, given that the initial states $\boldsymbol{X}(0)$ are within Ω.

C. Energy Function Method

Energy function methods are well-suited to evaluate transient stability, by which high-dimension states are transformed into a single index of system energy [33]. If system energy is lower than the critical energy, system states will stay in the stability region. The critical energy corresponds to stability boundary and its accurate computation is nontrivial. The theoretical foundation for critical energy can be found in [33].

The corresponding energy function for (1) is as follows [34]:

$$\begin{aligned} H = {} & \frac{1}{2}\sum_{i=1}^{n} M_i\omega_N\omega_i^2 + \sum_{i=1}^{n} P_i(\delta_{is}-\delta_i) \\ & + \left[\sum_{i=1}^{n}\sum_{j=i+1}^{n} E_iE_jB_{ij}\cos(\delta_{is}-\delta_{js})\right. \\ & \left. - \sum_{i=1}^{n}\sum_{j=i+1}^{n} E_iE_jB_{ij}\cos(\delta_i-\delta_j)\right] \end{aligned} \tag{3}$$

where δ_{is} and δ_{js} denote the equilibrium rotor angle of the ith and jth generators, respectively.

Accordingly, the stability probability can be calculated by the following form:

$$P(t|H_0) = P\{H(\tau) < H_{cr}, \tau \in (0,t]|H(0) = H_0 < H_{cr}\} \tag{4}$$

where $P(t\,|\,H_0)$ is the conditional probability of $H(t)$ being lower than the critical energy H_{cr} within the time interval $[0,\ t)$, given that the initial value H_0 is lower than H_{cr}.

In the following, an analytical method for calculating stability probability will be presented in detail.

IV. Analytical Assessment Method Based on Stochastic Averaging for Transient Stability Under Stochastic Continuous Disturbances

The stochastic averaging method (SAM) is an effective approximation method for nonlinear stochastic system analysis. SAM was proposed to obtain the simplified model when the system is a quasi-Hamiltonian system [32]. In many nonlinear stochastic dynamical systems of engineering interest, the response quantities can often be distinguished into two classes of different time scales: Rapidly varying ones and slowly varying ones. For instance, in the power system (1), there may be an exchange between the potential energy (corresponding to the rotor angle) and kinetic energy (corresponding to the rotor speed deviation), when the total energy is almost constant. As a consequence, system states (the rotor angle and rotor speed deviation) are rapidly varying quantities while the system energy is a slowly varying quantity (corresponding to system states). Via SAM, one averages rapidly varying quantities to derive the approximate differential equations of the slowly varying quantities, which are much simpler and of fewer dimension than the original equations. In the following, the analytical assessment method based on stochastic averaging will be presented for stochastic transient stability assessment under stochastic continuous disturbances.

A. Stochastic Model in Quasi-Hamiltonian Form

To apply SAM, the stochastic model should be expressed in the quasi-Hamiltonian form [32]. Stochastic model in quasi-Hamiltonian form for (1) is as follows:

$$\begin{cases} d\delta_i = \frac{1}{M_i}\frac{\partial H}{\partial \omega_i}\mathrm{d}t \\ d\omega_i = \left(-\frac{1}{M_i}\frac{\partial H}{\partial \delta_i} - \frac{D_i}{{M_i}^2\omega_N}\frac{\partial H}{\partial \omega_i}\right)\mathrm{d}t + \frac{\sigma_i}{M_i}\mathrm{d}B_i(t) \\ \qquad i = 1,2,\ldots,n \end{cases} \tag{5}$$

where ∂ is the partial differential operator; $B_i(t)$ are Wiener processes and $\mathrm{d}B_i(t)/\mathrm{d}t = W_i(t)$.

Based on Itō formula [35], Itō equation of system energy H can be expressed as follows:

$$\begin{aligned} \mathrm{d}H = {} & \sum_{i-1}^{n}\left\{\frac{\partial H}{\partial \omega_i}\left[\left(-\frac{1}{M_i}\frac{\partial H}{\partial \delta_i} - \frac{D_i}{{M_i}^2\omega_N}\frac{\partial H}{\partial \omega_i}\right)\mathrm{d}t\right.\right. \\ & \left. + \frac{\sigma_i}{M_i}\mathrm{d}B_i(t)\right] \\ & \left. + \frac{1}{M_i}\frac{\partial H}{\partial \delta_i}\frac{\partial H}{\partial \omega_i}\mathrm{d}t + \frac{1}{2}\frac{{\sigma_i}^2}{{M_i}^2}\frac{\partial^2 H}{\partial {\omega_i}^2}\mathrm{d}t\right\} \\ = {} & \sum_{i=1}^{n}\left[-D_i\omega_N{\omega_i}^2 + \frac{{\sigma_i}^2\omega_N}{2M_i}\right]\mathrm{d}t + \sum_{i=1}^{n}\sigma_i\omega_N\omega_i\mathrm{d}B_i(t). \end{aligned} \tag{6}$$

B. Stochastic Averaging Method

Based on a lemma of Khasminskii [32], system energy H weakly converges to a first-order diffusion process, as follows:

$$\mathrm{d}H = m^*(H)\mathrm{d}t + \sigma^*(H)\mathrm{d}B(t). \tag{7}$$

The coefficients $m^*(H)$ and $\sigma^*(H)$ can be obtained by time-averaging, where

$$\begin{cases} m^*(H) = \lim\limits_{T\to\infty}\dfrac{1}{T}\int_0^T\sum_{i=1}^{n}\left(-D_i\omega_N{\omega_i}^2 + \dfrac{{\sigma_i}^2\omega_N}{2M_i}\right)\mathrm{d}t \\ \sigma^{*2}(H) = \lim\limits_{T\to\infty}\dfrac{1}{T}\int_0^T\sum_{i=1}^{n}\left(\sigma_i\omega_N\omega_i\right)^2\mathrm{d}t \end{cases}. \tag{8}$$

It is difficult to calculate time-averaging results ($m^*(H)$ and $\sigma^{*2}(H)$) from (8) directly because system states ω_i are unknown at a given time.

Due to the ergodicity of Hamiltonian system, the following three hypotheses of ergodicity can be adopted to

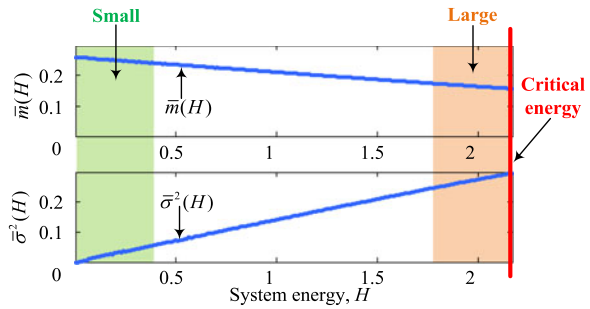

Fig. 3. Coefficients changing with system energy H.

calculate the time-averaging results [32], [36], [37]: 1) time-averaging results are equal to corresponding space-averaging results in the space $\Omega = \{(\Delta\delta_1, \ldots, \Delta\delta_{n-1}, \omega_1, \ldots, \omega_n) | H(\Delta\delta_1, \ldots, \Delta\delta_{n-1}, \omega_1, \ldots, \omega_n) = H\}$, where $\Delta\delta_i = \delta_i - \delta_n$ (the nth generator is regarded as a reference node); 2) system states can arrive everywhere in Ω; furthermore, 3) for any given energy level H, the conditional probabilities of different system state in Ω are equal. Let $\mathrm{d}s/S$ denote the probability of states being in a certain small piece, where S is the surface area of whole hypersphere Ω and $\mathrm{d}s$ is the surface area of a certain small piece of the hypersphere Ω. Then, space-averaging results, which are equal to time-averaging results, can be deduced as follows:

$$\begin{cases} \bar{m}(H) = \frac{1}{S}\int_\Omega \sum_{i=1}^n \left(-D_i {\omega_N \omega_i}^2 + \frac{{\sigma_i}^2 \omega_N}{2M_i}\right)\mathrm{d}s \\ \bar{\sigma}^2(H) = \frac{1}{S}\int_\Omega \sum_{i=1}^n (\sigma_i \omega_N \omega_i)^2 \mathrm{d}s \\ S = \int_\Omega 1 \mathrm{d}s \end{cases} \tag{9}$$

where $\int$ denotes the surface integral operator; Ω denotes the integral domain.

Accordingly, the first-order diffusion process of system energy becomes:

$$\mathrm{d}H = \bar{m}(H)\mathrm{d}t + \bar{\sigma}(H)\mathrm{d}B(t) \tag{10}$$

where $\bar{m}(H)$ and $\bar{\sigma}(H)$ are the drift coefficient and diffusion coefficient, respectively.

C. Linear Relation in Stochastic Averaging

Based on many simulations for stochastic averaging results of (9), it is found that the relation between coefficients (i.e., $\bar{m}(H)$ and $\bar{\sigma}(H)$) and energy H is approximately linear, even though the original system is nonlinear. For instance, in the Kundur's 4-machine 2-area system, the stochastic averaging results are shown in Fig. 3. Clearly, the linear relation exists even when the system energy is close to critical energy.

The stochastic continuous disturbances are usually smaller than system faults, which is one of the reasons that linear relation exists. It is known that a power system shows nonlinearity when a severe system fault occurs. The stability analysis under a severe system fault is a nonlinear problem because the system fault is large and instant. However, a novel instability mechanism works in the system under stochastic continuous disturbances, which describes that the random effects of small stochastic continuous disturbances "can cause the trajectories of the system to leave any bounded domain with probability one" [15], even the stable domain; see also [16], [17].

The linear relation suggests that coefficients $\bar{m}(H)$ and $\bar{\sigma}(H)$ can be expressed by simple equations, which are shown as follows:

$$\begin{cases} \bar{m}(H) = a - bH \\ \bar{\sigma}^2(H) = cH \end{cases}. \tag{11}$$

In (11), a, b, and c are constant whether H is large or small. A small deviation of H means the system is subjected to small disturbances. Therefore, a linearized model based on small disturbances can be used to calculate a, b, and c, which are derived as follows (the derivation is presented in Appendix A):

$$\begin{cases} \bar{m}(H) = \left(\sum_{i=1}^n \frac{\omega_N {\sigma_i}^2}{2M_i}\right) - \left[\sum_{i=1}^n \frac{2D_i}{M_i(2n-1)}\right] H \\ \bar{\sigma}^2(H) = \left[\sum_{i=1}^n \frac{2\omega_N {\sigma_i}^2}{M_i(2n-1)}\right] H \end{cases}. \tag{12}$$

By adopting the linear relation in SAM, one can obtain clearer results, but it does not mean that the linear relation is necessary for SAM. The analytical assessment method still works without using the linear relation. In this study, when the linear relation is not adopted, the dynamic function of system energy function can also be deduced by SAM, which is shown in (9).

D. Analytical Results of Stability Probability

In stochastic theory, the stability probability shown in (2) is defined as the reliability of diffusion process (10), which can be solved by Kolmogorov's backward equation as follows [38]:

$$\frac{\partial P(t|H_0)}{\partial t} = \bar{m}(H_0)\frac{\partial P(t|H_0)}{\partial H_0} + \frac{\bar{\sigma}(H_0)^2}{2}\frac{\partial^2 P(t|H_0)}{\partial {H_0}^2}. \tag{13}$$

Equation (13) is a parabolic partial differential equation. A solution of a partial differential equation is not unique generally, so additional conditions must be specified on the boundary of the region where the solution is defined. The initial conditions and boundary conditions for (13) are as follows:

$$\begin{cases} \text{Initial condition}: \text{ if } H_0 < H_{cr},\ P(0|H_0) = 1 \\ \text{Boundary condition 1}: \ P(t|H_{cr}) = 0 \\ \text{Boundary condition 2}: \text{if } H_0 = 0,\ \frac{\partial P}{\partial t} = \bar{m}(0)\frac{\partial P}{\partial H_0} \end{cases} \tag{14}$$

where the initial condition denotes that stability probability P at $t = 0s$ equals 1, when the initial energy H_0 is lower than the critical energy H_{cr}; boundary condition 1 denotes that stability probability P is equal to 0, if the initial energy H_0 is higher than the critical energy H_{cr}; boundary condition 2 denotes that the solution at $H_0 = 0$ should satisfy $\frac{\partial P}{\partial t} = \bar{m}(0)\frac{\partial P}{\partial H_0}$, which is used to assure the solution with initial energy H_0 being higher than 0.

Several numerical calculation methods can be used to solve (13), such as the finite difference method. In this study, the finite difference method based on Crank Nicholson's scheme is applied. Detailed procedures of the scheme can be found in [38].

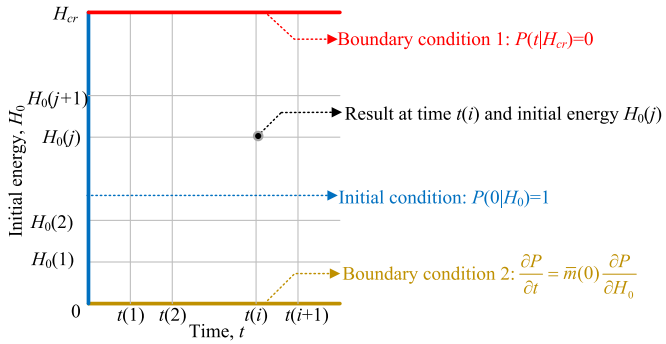

Fig. 4. The discrete result mesh of Kolmogorov's backward equation.

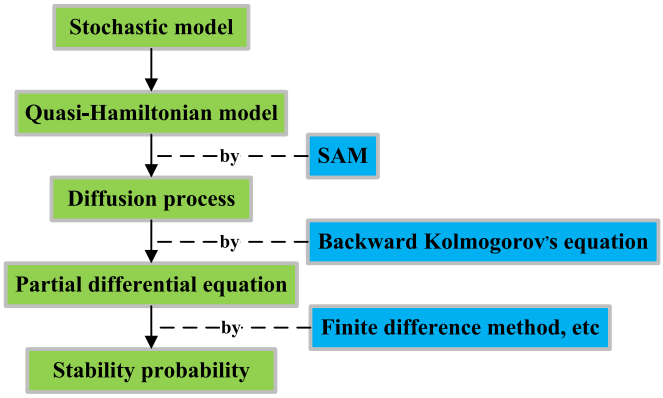

Fig. 5. The procedure of the analytical assessment method.

To illustrate the solution of (13) clearly, Fig. 4 shows the discrete result mesh for Kolmogorov's backward equation. By the finite difference method, consider $P(t|H_0)$ only at discrete time values $t(i) = i\Delta t\,(i = 0, 1, 2, \ldots)$ and discrete initial energy values $H_0(j) = j\Delta H_0\,(j = 0, 1, 2, \ldots)$. Then $t(i)$ and $H_0(j)$ constitute a discrete result mesh in the plane $(t,\ H_0)$. Also, it can be seen that the initial conditions and boundary conditions define the region for the solution of (13).

E. Application to Realistic Model

In this section, a systematic strategy of applying SAM to assess transient stability under stochastic continuous disturbances is provided. Even though the classical model is often used in transient stability assessment, more realistic models are desired in practice. Theoretically, one can utilize SAM [32], [36], [37], if the power system model can be expressed in a Hamiltonian form. In recent years, much research on modeling realistic power system as the Hamiltonian model has been carried out [39]–[42]. Considering the above analysis, the application of SAM to more realistic model is feasible theoretically. For power systems which can be expressed in the quasi-Hamiltonian form, the procedure of the proposed analytical assessment method is outlined below and shown in Fig. 5.

Step 1: Build the stochastic model.

Step 2: Express the model in quasi-Hamiltonian form.

Step 3: Deduce the diffusion equation of system energy based on SAM.

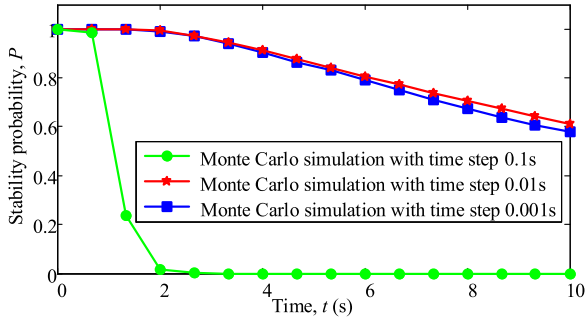

Fig. 6. Monte Carlo simulation results under time step 0.1 s, 0.01 s, and 0.001 s.

Step 4: Obtain the partial differential equation of stability probability by using backward Kolmogorov's equation.

Step 5: Calculate stability probability from the partial differential equation by numerical calculation methods.

V. Validations

All the simulations are conducted on a computer running a 64-bit Windows 10, with a 2.69 GHz Intel I7-4600U CPU and 8 GB memory.

A. Monte Carlo Simulation for Stability Probability

To verify the accuracy and efficiency of the proposed method, Monte Carlo simulation results are used as a reference. In Monte Carlo simulation, proper iteration and time step are of great concern. One can get more (less) accurate results with a larger (smaller) iteration and smaller (larger) time step, but it takes more (less) time. In most Monte Carlo simulations, it is difficult to specify a proper number of iterations and time step directly, so the additional studies to choose the number of iterations and time step need to be carried out. From the aspect of choosing the time step and number of iterations, the proposed analytical method is better, because researchers need not choose the number of iterations and time step, which means the proposed method is 'ready to use'.

Fig. 6 shows three Monte Carlo simulation results (stability probability curves) with time step 0.1 s, 0.01 s, and 0.001 s in the Kundur's 4-machine 2-area system. Clearly, the stability probability curve with time step 0.1 s is much far from those with time step 0.01 s and 0.001 s, which means that time step 0.1 s is too large for Monte Carlo simulation in this study. Moreover, the stability probability curve with time step 0.01 s agrees well with that with time step 0.001 s. Hence, time step 0.01 s is chosen for Monte Carlo simulation in this study.

In Fig. 7, three cases of Monte Carlo simulation in the Kundur's 4-machine 2-area system with 500, 5000, and 50000 iterations are shown. Clearly, most Monte Carlo simulation results with 5000 iterations are close to those with 50000 iterations, which means the Monte Carlo simulation with 5000 iterations is relatively accurate. However, the performance of Monte Carlo simulation with 500 iterations degrades. Hence, several

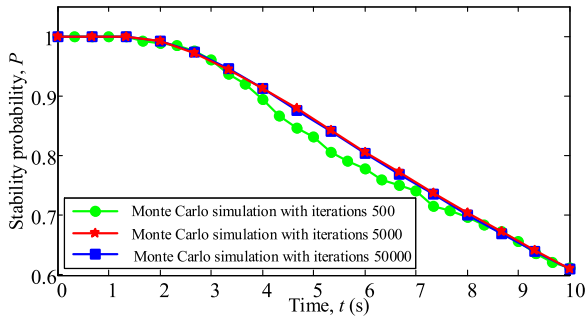

Fig. 7. Monte Carlo simulation results under iterations 500, 5000, and 50000.

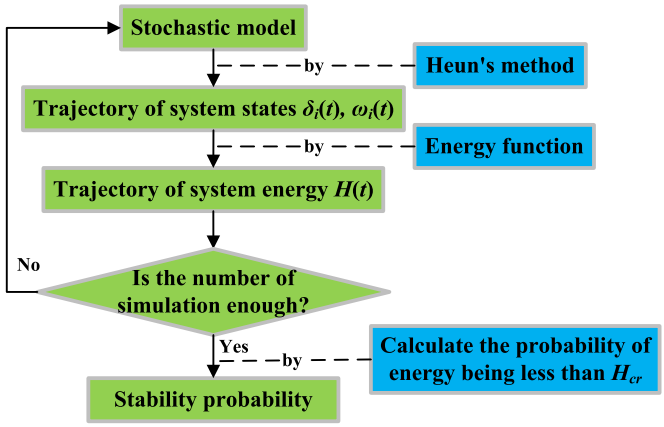

Fig. 8. The procedure of Monte Carlo simulation.

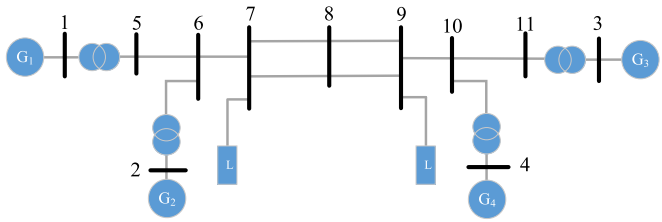

Fig. 9. Kundur's 4-machine 2-area power system.

thousands of iterations are proper for the Monte Carlo simulation in this study.

The procedure of Monte Carlo simulation for calculating the stability probability is outlined below and shown in Fig. 8.

Step 1: Calculate system states trajectories by a single simulation.

Step 2: Calculate system energy trajectories based on system states trajectories.

Step 3: Execute Step 1 and Step 2 repeatedly, if the number of simulation is not enough; go to Step 4, if the number of simulation is enough.

Step 4: Calculate the probability of system energy being less than critical energy $H_{\rm cr}$.

B. Accuracy Comparisons

The Kundur's 4-machine 2-area system, which is shown in Fig. 9, is adopted as the first simulation system. The system

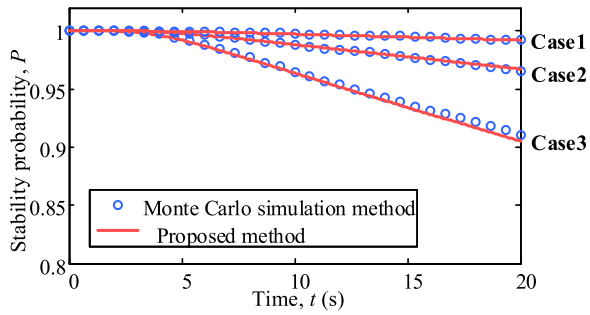

Fig. 10. Stability probability curves of Kundur's 4-machine 2-area power system under stochastic continuous disturbances.

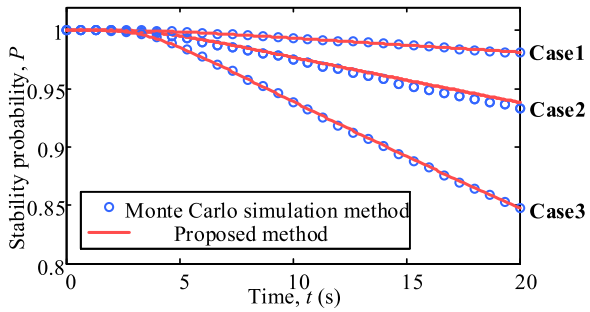

Fig. 11. Stability probability curves of a 50-machine 145-bus test power system under stochastic continuous disturbances.

is reduced to a 4-bus system by eliminating all the load buses. Then, the system is simulated with the integration of stochastic continuous disturbances, which are represented as Gauss white noises with intensities of σ_1, σ_2, σ_3, and σ_4, at Generator 1, Generator 2, Generator 3, and Generator 4, respectively. The network and generator's parameters are the same as in [34].

In this case study, the transient stability under stochastic continuous disturbances is investigated by utilizing the proposed method, and results are compared with Monte Carlo simulation results. Three simulation cases with different disturbance intensity are demonstrated: Case1: $\sigma_1 = \sigma_2 = \sigma_3 = \sigma_4 = 0.07$; Case2: $\sigma_1 = \sigma_2 = \sigma_3 = \sigma_4 = 0.075$; Case3: $\sigma_1 = \sigma_2 = \sigma_3 = \sigma_4 = 0.08$. Fig. 10 shows the stability probability curves solved by the proposed method and Monte Carlo simulation. It can be seen that the analytical results are very close to Monte Carlo simulation results.

A 50-machine 145-bus test power system is also used to demonstrate the effectiveness of the proposed method. The system is reduced to a 50-bus system by eliminating load buses. Assume that all generators are subjected to stochastic continuous disturbances with the same intensity. Three cases with different disturbance intensity are simulated: Case1: small intensity; Case2: medium intensity; Case3: large intensity. Results from the proposed method and Monte Carlo simulation are shown in Fig. 11. It can be seen that analytical results are still close to Monte Carlo simulation results, which demonstrates the applicability of the proposed method in bulk power systems.

TABLE I
COMPUTATIONAL TIME COMPARISONS OF MONTE CARLO SIMULATION AND THE PROPOSED METHOD

Number of generators	Computational Time, t (s)	
	Monte Carlo simulation	Proposed method
4	42.9	0.1
10	151.7	0.1
16	387.1	0.1
50	4193.2	0.1

C. Computational Time Comparisons

The computational efficiency is also important in practice. When the simulation time t is set as 20 s, computational time comparisons of the Monte Carlo simulation and the proposed method are operated based on four power systems with a different number of generators, as shown in Table I.

In Table I, computational time of Monte Carlo simulation is almost a quadratic power function with the number of generators, while that of the proposed method is much smaller and nearly constant with the increasing of the number of generators. It is easy to understand that the proposed method is much faster than Monte Carlo simulation, due to no iterative computations.

The high efficiency makes the proposed method very attractive when many plans for transient stability must be compared or when transient stability must be analyzed quickly for a multi-machine power system.

D. Visualization of the Stability Probability

To give a good indication of how stochastic continuous disturbances impact transient stability, the visualization of stability probability is presented in this section. The stability probability strongly depends on disturbance intensities and damping coefficients, so the visualization is used to illustrate stability probabilities changes with varied disturbance intensities and varied damping coefficients. The proposed method is adopted for solving the stability probability of Kundur's 4-machine 2-area system under stochastic continuous disturbances again. For simplicity, let all the damping coefficients (and all disturbance intensities) in the system increase or decrease with the same degree, which is described as damping level (and disturbance intensity level). For example, a damping level of 110% means all damping coefficients increase to 110%. Fig. 12 shows stability probability curves under different damping levels and fixed other parameters at time $t = 20$ s. Fig. 13 shows stability probability curves under different disturbance intensity levels and fixed other parameters at time $t = 20$ s. Clearly, stability probability increases with the increasing of damping coefficient and the decreasing of disturbances intensity. Furthermore, a critical level shown corresponding to a stability probability of 0.99 is found, beyond which the increase of stability probability is very gradual. The systems are stable with high probability when the damping level is greater than the critical damping level (and the critical disturbance intensity level is lower than the critical disturbance intensity level).

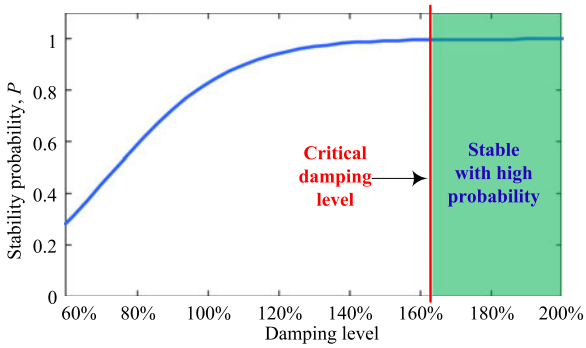

Fig. 12. Stability probability curves under different damping coefficient levels and fixed other parameters at time $t = 20$ s.

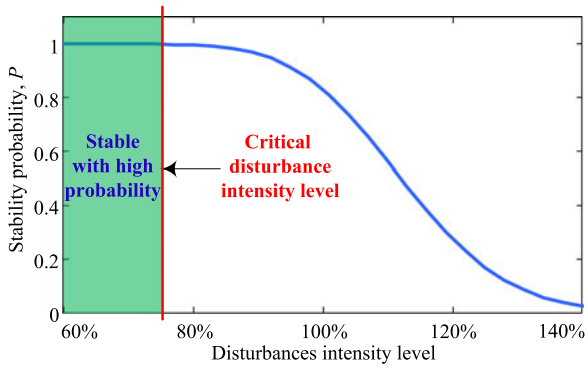

Fig. 13. Stability probability curves under different disturbance intensity levels and fixed other parameters at time $t = 20$ s.

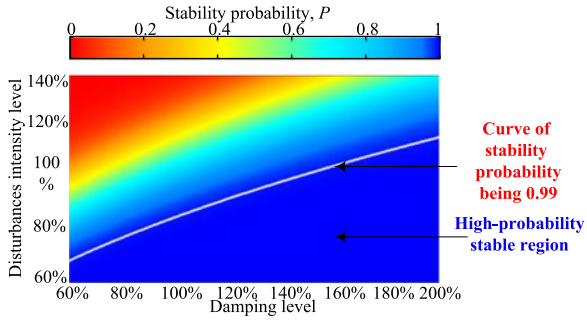

Fig. 14. Visual illustration of the high-probability stable regions.

In above analysis, only damping level or disturbance intensity level is varied, but both damping level and disturbance intensity level are varied over time in actual power systems. Fig. 14 shows the stability probability under varied damping and varied disturbance intensity levels at time $t = 20$ s. A stable region with the stability probability is over 0.99 is found, in which the change of stability probability is very gradual. The high-probability stable region is visually illustrated as a domain of disturbance intensity level and damping level. To enhance the stability under stochastic continuous disturbances, it would be a useful technique keeping the operation level within the high-probability stable region. Based on the visualization of stability probability, it is easier to answer questions when the stochastic continuous disturbances need to be considered in transient stability study,

whether the system is stable with high probability, and how to improve stability under stochastic continuous disturbances.

VI. Conclusion

Due to the increasing stochastic continuous disturbances, power system transient stability is of concern. This paper provides an analytical assessment method for power system transient stability under stochastic continuous disturbances, in which there are four main contributions:

1) Stability probability is presented as a measure of transient stability under stochastic continuous disturbances;
2) An analytical assessment method based on stochastic averaging is proposed for solving stability probability;
3) The evolution of system energy over time is found as a simple diffusion process;
4) The combined impacts of damping level and disturbance intensity level on transient stability are visualized.

With the challenges of stochastic continuous disturbances, an accurate and efficient assessment tool for transient stability is desired. We believe that the proposed method will serve well in this regard.

Appendix A

A. Linearization of Stochastic Model and Energy Function

According to model (1), the linearized stochastic model can be derived as follows [43]:

$$\begin{cases} \dfrac{\mathrm{d}\Delta\delta_i}{\mathrm{d}t} = \omega_N \Delta\omega_i & i = 1, 2, \ldots, n-1 \\ M_i \dfrac{\mathrm{d}\Delta\omega_i}{\mathrm{d}t} = -\sum_{j=1, j\neq i}^{n} C_{ij}\left(\Delta\delta_i - \Delta\delta_j\right) - D_i\Delta\omega_i + \sigma_i W_i\left(t\right) & i = 1, 2, \ldots, n \end{cases} \tag{A-1}$$

where $\Delta\omega_i = \omega_i$; $\Delta\delta_i = \delta_i - \delta_n - \delta_{is} + \delta_{ns}$ and $\Delta\delta_n = 0$; δ_n is the rotor angle of nth generator, which is set as the reference node; and $C_{ij} = E_i E_j B_{ij}\cos(\delta_{is} - \delta_{js})$.

The linearized energy function is as follows:

$$H = \frac{1}{2}\sum_{i=1}^{n} M_i\omega_N {\Delta\omega_i}^2 + \frac{1}{2}\sum_{i=1}^{n}\sum_{j=i+1}^{n} C_{ij}(\Delta\delta_i - \Delta\delta_j)^2. \tag{A-2}$$

B. Linearized Energy Function in Matrix Form

System energy (A-2) can be expressed as follows:

$$H = \boldsymbol{X}^T\boldsymbol{Q}\boldsymbol{X} \tag{A-3}$$

where $\boldsymbol{X} = (\Delta\delta_1, \ldots, \Delta\delta_{n-1}, \Delta\omega_1, \ldots, \Delta\omega_n)^T$; $\boldsymbol{Q}$ is a $(2n-1)^{th}$-order positive definite matrix with the form

$$\boldsymbol{Q} = \left(\begin{array}{c|c} \boldsymbol{Q}_{11} & \boldsymbol{O} \\ \hline \boldsymbol{O} & \boldsymbol{Q}_{22} \end{array}\right) \tag{A-4}$$

where $\boldsymbol{Q}_{11}$ is an $(n-1)$th-order nonsingular symmetric matrix; $\boldsymbol{Q}_{22}$ is a nth-order diagonal matrix with the form $\boldsymbol{Q}_{22} = \mathrm{diag}(M_1\omega_N/2, \ldots, M_n\omega_N/2)$; and $\boldsymbol{O}$ denotes a null matrix.

Differentially (A-3), one obtains [44]

$$\begin{cases} \partial H/\partial \boldsymbol{X} = 2\boldsymbol{Q}\boldsymbol{X} \\ \partial^2 H/\partial \boldsymbol{X}^2 = 2\boldsymbol{Q} \end{cases} \tag{A-5}$$

where $\partial H/\partial \boldsymbol{X}$ is a $(2n-1)^{th}$-order column vector and $\partial H/\partial \boldsymbol{X} = (\partial H/\partial\Delta\delta_1, \ldots, \partial H/\partial\Delta\delta_{n-1} \quad \partial H/\partial\Delta\omega_1, \ldots, \partial H/\partial\Delta\omega_n)^T$; $\partial^2 H/\partial \boldsymbol{X}^2$ is a $(2n-1)^{th}$-order square matrix, in which the element in i^{th} row and jth column is $\partial^2 H/\partial x_i\partial x_j$. x_i and x_j denote the ith and jth element of $\boldsymbol{X}$, respectively.

C. Linearized Quasi-Hamiltonian Model in Matrix Form

According to (5), the linearized stochastic model in quasi-Hamiltonian form is as follows:

$$\mathrm{d}\boldsymbol{X} = \boldsymbol{M}\partial H/\partial \boldsymbol{X}\mathrm{d}t + \boldsymbol{D}\partial H/\partial \boldsymbol{X}\mathrm{d}t + \boldsymbol{G}\mathrm{d}\boldsymbol{B}\left(t\right) \tag{A-6}$$

where $\mathrm{d}\boldsymbol{X} = (\mathrm{d}\Delta\delta_1, \ldots, \mathrm{d}\Delta\delta_{n-1}, \mathrm{d}\Delta\omega_1, \ldots, \mathrm{d}\Delta\omega_n)^T$; $\mathrm{d}\boldsymbol{B}(t) = [\mathrm{d}B_1(t), \ldots, \mathrm{d}B_i(t), \ldots, \mathrm{d}B_{2n-1}(t)]^T$ and $\mathrm{d}B_i(t)$ is independent under different i; $\boldsymbol{M}$, $\boldsymbol{D}$, and $\boldsymbol{G}$ are $(2n-1)^{th}$-order square matrices; $\boldsymbol{M}$ describes the characteristic of system conservation and $\boldsymbol{M} + \boldsymbol{M}^T = O$; $\boldsymbol{D}$ describes the characteristic of system dissipation and is a $(2n-1)^{th}$-order diagonal matrix $\mathrm{diag}(0, \ldots, 0, -D_1/\omega_N M_1^2, \ldots, -D_n/\omega_N M_n^2)$; G denotes the intensity of stochastic continuous disturbances and is a $(2n-1)^{th}$-order diagonal matrix $\mathrm{diag}(0, \ldots, 0, \sigma_1/M_1, \ldots, \sigma_n/M_n)$.

Combining (A-5) and (A-6), one has

$$\mathrm{d}\boldsymbol{X} = 2\boldsymbol{M}\boldsymbol{Q}\boldsymbol{X}\mathrm{d}t + 2\boldsymbol{D}\boldsymbol{Q}\boldsymbol{X}\mathrm{d}t + \boldsymbol{G}\mathrm{d}\boldsymbol{B}\left(t\right). \tag{A-7}$$

D. Standard Quadric Form of the Energy Function and Linear Transformation

Given that $\boldsymbol{Q}$ in (A-4) is a positive definite matrix, the linearized energy function (A-3) can be transformed into the following standard quadric form

$$H = \boldsymbol{Y}^T\boldsymbol{Y} = {y_1}^2 + \cdots {y_i}^2 \cdots + {y_{2n-1}}^2 \tag{A-8}$$

where $\boldsymbol{Y} = (y_1, \ldots, y_i, \ldots, y_{2n-1})^T$, $\boldsymbol{Y} = \boldsymbol{C}X$, $\boldsymbol{Q} = \boldsymbol{C}^T C$, and $\boldsymbol{C}$ is a non-singular matrix with $(2n-1)^{th}$-order. Due to the special form of $\boldsymbol{Q}$, $\boldsymbol{C}$ has the form of

$$\boldsymbol{C} = \left(\begin{array}{c|c} \boldsymbol{C}_{11} & \boldsymbol{O} \\ \hline \boldsymbol{O} & \boldsymbol{C}_{22} \end{array}\right) \tag{A-9}$$

where $\boldsymbol{C}_{11}$ is an $(n-1)^{th}$-order non-singular matrix and $\boldsymbol{C}_{22}$ is a nth-order diagonal matrix $\mathrm{diag}(\sqrt{M_1\omega_N/2}, \ldots, \sqrt{M_n\omega_N/2})$.

Differentially (A-8), one obtains [44]

$$\begin{cases} \partial H/\partial \boldsymbol{Y} = 2\boldsymbol{Y} \\ \partial^2 H/\partial \boldsymbol{Y}^2 = 2\boldsymbol{E} \end{cases} \tag{A-10}$$

where $\boldsymbol{E}$ is a $(2n-1)^{th}$-order unit matrix.

Using $\boldsymbol{Y} = \boldsymbol{C}X$ and $\boldsymbol{Q} = \boldsymbol{C}^T C$, (A-7) is transformed as follows:

$$\mathrm{d}\boldsymbol{Y} = \boldsymbol{C}\mathrm{d}\boldsymbol{X} = 2\boldsymbol{C}\boldsymbol{M}\boldsymbol{C}^T\boldsymbol{Y}\mathrm{d}t + 2\boldsymbol{C}\boldsymbol{D}\boldsymbol{C}^T\boldsymbol{Y}\mathrm{d}t + \boldsymbol{C}\boldsymbol{G}\mathrm{d}\boldsymbol{B}\left(t\right). \tag{A-11}$$

E. Stochastic Averaging of Energy Function

Based on Itō formula [35], Itō equation of system energy (A-8) can be expressed as follows:

$$\begin{aligned}\mathrm{d}H &= (\partial H/\partial \boldsymbol{Y})^T \mathrm{d}\boldsymbol{Y} + (1/2)tr(\boldsymbol{C}\boldsymbol{G}\boldsymbol{G}^T\boldsymbol{C}^T\partial^2 H/\partial \boldsymbol{Y}^2)\mathrm{d}t \\ &= 4\boldsymbol{Y}^T\boldsymbol{C}\boldsymbol{D}\boldsymbol{C}^T\boldsymbol{Y}\mathrm{d}t + tr(\boldsymbol{C}\boldsymbol{G}\boldsymbol{G}^T\boldsymbol{C}^T)\mathrm{d}t \\ &\quad + 2\boldsymbol{Y}^T\boldsymbol{C}\boldsymbol{G}\mathrm{d}\boldsymbol{B}(t) \end{aligned} \tag{A-12}$$

where $tr(\boldsymbol{C}\boldsymbol{G}\boldsymbol{G}^T\boldsymbol{C}^T)$ is the trace of matrix $\boldsymbol{C}\boldsymbol{G}\boldsymbol{G}^T\boldsymbol{C}^T$ (i.e., the summation of all diagonal elements in $\boldsymbol{C}\boldsymbol{G}\boldsymbol{G}^T\boldsymbol{C}^T$).

One can derive the following equations easily:

$$\begin{cases} \boldsymbol{C}\boldsymbol{D}\boldsymbol{C}^T = \mathrm{diag}[0,\cdots,0,-D_1/(2M_1),\cdots,-D_n/(2M_n)] \\ \boldsymbol{C}\boldsymbol{G}\boldsymbol{G}^T\boldsymbol{C}^T = \mathrm{diag}[0,\cdots,0,\omega_N{\sigma_1}^2/(2M_1),\cdots, \\ \quad \times \omega_N{\sigma_n}^2/(2M_n)] \\ \boldsymbol{C}\boldsymbol{G} = \mathrm{diag}[0,\cdots,0,\sigma_1\sqrt{\omega_N/(2M_1)},\cdots, \\ \quad \times \sigma_n\sqrt{\omega_N/(2M_n)}] \end{cases} \tag{A-13}$$

Combining (A-12) and (A-13), one obtains

$$\begin{aligned}\mathrm{d}H &= \sum_{i=1}^{n}\left(\frac{-2D_i}{M_i}{y_{n-1+i}}^2 + \frac{{\sigma_i}^2\omega_N}{2M_i}\right)\mathrm{d}t \\ &\quad + \sum_{i=1}^{n}\left[\sigma_i\sqrt{\frac{2\omega_N}{M_i}}y_{n-1+i}\mathrm{d}B_i(t)\right] \\ &= \sum_{i=1}^{n}\left(\frac{-2D_i}{M_i}{y_{n-1+i}}^2 + \frac{{\sigma_i}^2\omega_N}{2M_i}\right)\mathrm{d}t \\ &\quad + \sqrt{\sum_{i=1}^{n}\left(\frac{2\omega_N{\sigma_i}^2}{M_i}{y_{n-1+i}}^2\right)}\mathrm{d}B(t). \end{aligned} \tag{A-14}$$

According to the stochastic averaging results shown in (9), system energy H weakly converges to the first-order diffusion process as follows:

$$\mathrm{d}H = \bar{m}(H)\mathrm{d}t + \bar{\sigma}(H)\mathrm{d}B(t) \tag{A-15}$$

where

$$\begin{cases} \bar{m}(H) = \frac{1}{S}\int_\Omega \sum_{i=1}^{n}\left(\frac{-2D_i}{M_i}{y_{n-1+i}}^2 + \frac{{\sigma_i}^2\omega_N}{2M_i}\right)\mathrm{d}s \\ \qquad = \sum_{i=1}^{n}\left(\frac{{\sigma_i}^2\omega_N}{2M_i}\right) - \sum_{i=1}^{n}\left(\frac{2D_i}{M_i}\cdot\frac{\int_\Omega {y_{n-1+i}}^2\mathrm{d}s}{\int_\Omega 1\mathrm{d}s}\right) \\ \bar{\sigma}^2(H) = \frac{1}{S}\int_\Omega \sum_{i=1}^{n}\left(\frac{2\omega_N{\sigma_i}^2}{M_i}{y_{n-1+i}}^2\right)\mathrm{d}s \\ \qquad = \sum_{i=1}^{n}\left(\frac{2\omega_N{\sigma_i}^2}{M_i}\cdot\frac{\int_\Omega {y_{n-1+i}}^2\mathrm{d}s}{\int_\Omega 1\mathrm{d}s}\right) \\ S = \int_\Omega 1\mathrm{d}s \\ \Omega = \left\{(y_1,\cdots,y_i,\cdots,y_{2n-1})\middle|\, {y_1}^2+\cdots {y_i}^2\cdots \right. \\ \quad \left. + {y_{2n-1}}^2 = H\right\} \end{cases} \tag{A-16}$$

F. Symmetry of First Type Surface Integral

Using the symmetry of the first type surface integral [45], one has

$$\int_\Omega {y_1}^2\mathrm{d}s = \cdots = \int_\Omega {y_i}^2\mathrm{d}s = \cdots = \int_\Omega {y_{2n-1}}^2\mathrm{d}s. \tag{A-17}$$

According to the energy function (A-8), the following equation can be deduced

$$\sum_{i=1}^{2n-1}\int_\Omega {y_i}^2\mathrm{d}s = \int_\Omega \sum_{i=1}^{2n-1}{y_i}^2\mathrm{d}s = \int_\Omega H\mathrm{d}s = H\int_\Omega 1ds. \tag{A-18}$$

Combining (A-18) and (A-17), one obtains

$$\frac{\int_\Omega {y_i}^2\mathrm{d}s}{\int_\Omega 1\mathrm{d}s} = \frac{H}{(2n-1)}. \tag{A-19}$$

By incorporating (A-19) into (A-16), the following equations can be deduced

$$\begin{cases} \bar{m}(H) = \left(\sum_{i=1}^{n}\frac{\omega_N{\sigma_i}^2}{2M_i}\right) - \left[\sum_{i=1}^{n}\frac{2D_i}{M_i(2n-1)}\right]\cdot H \\ \bar{\sigma}^2(H) = \left[\sum_{i=1}^{n}\frac{2\omega_N{\sigma_i}^2}{M_i(2n-1)}\right]\cdot H \end{cases} \tag{A-20}$$

ACKNOWLEDGMENT

The authors gratefully acknowledge Dr. Weiqiu Zhu for his guidance. The authors also would like to thank Dr. Robert Mee for his discussions on this research.

REFERENCES

[1] J. D. McCalley *et al.*, "Probabilistic security assessment for power system operations," in *Proc. IEEE Power Eng. Soc. General Meeting*, 2004, pp. 212–220.

[2] R. Billinton and P. R. S. Kuruganty, "A probabilistic index for transient stability," *IEEE Trans. Power App. Syst.*, vol. PAS-99, no. 1, pp. 195–206, Jan. 1980.

[3] P. Rezaei, P. Hines, and M. Eppstein, "Estimating cascading failure risk with random chemistry," *IEEE Trans. Power Syst.*, vol. 30, no. 5, pp. 2726–2735, Sep. 2015.

[4] A. Salehi-Dobakhshari and M. Fotuhi-Firuzabad, "Integration of large-scale wind farm projects including system reliability analysis," *IET Renewable Power Gener.*, vol. 5, no. 1, pp. 89–98, Jan. 2011.

[5] C. Zhang and J. Wang, "Optimal transmission switching considering probabilistic reliability," *IEEE Trans. Power Syst.*, vol. 29, no. 2, pp. 974–975, Mar. 2014.

[6] C. Wang, K. Yuan, P. Li, B. Jiao, and G. Song, "A projective integration method for transient stability assessment of power systems with a high penetration of distributed generation," *IEEE Trans. Smart Grid*, to be published.

[7] S. Liu, X. Wang, and P. Liu, "A stochastic stability enhancement method of grid-connected distributed energy storage systems," *IEEE Trans. Smart Grid*, to be published.

[8] W. Li, "Framework of probabilistic power system planning," *CSEE J. Power Energy Syst.*, vol. 1, no. 1, pp. 1–8, Mar. 2015.

[9] L. Xie *et al.*, "Wind integration in power systems: Operational challenges and possible solutions," *Proc. IEEE*, vol. 99, no. 1, pp. 214–232, Jan. 2011.

[10] S. Shen *et al.*, "An adaptive protection scheme for distribution systems with DGs based on optimized Thevenin equivalent parameters estimation," *IEEE Trans. Power Del.*, vol. 32, no. 1, pp. 411–419, Feb. 2017.

[11] A. J. Conejo, Y. Cheng, N. Zhang, and C. Kang, "Long-term coordination of transmission and storage to integrate wind power," *CSEE J. Power Energy Syst.*, vol. 3, no. 1, pp. 36–43, Mar. 2017.
[12] C. Gan, J. Wu, Y. Hu, S. Yang, W. Cao, and J. M. Guerrero, "New integrated multilevel converter for switched reluctance motor drives in plug-in hybrid electric vehicles with flexible energy conversion," *IEEE Trans. Power Electron.*, vol. 32, no. 5, pp. 3754–3766, May 2017.
[13] M. Liu, P. McNamara, R. Shorten and S. McLoone, "Residential electrical vehicle charging strategies: The good, the bad and the ugly," *J. Modern Power Syst. Clean Energy*, vol. 3, no. 2, pp. 190–202, Jun. 2015.
[14] Y. Xu, J. Ma, Z. Dong, and D. Hill, "Robust transient stability-constrained optimal power flow with uncertain dynamic loads," *IEEE Trans. Smart Grid*, vol. 8, no. 4, pp. 1911–1921, Jul. 2017.
[15] J. Qui, S. Shahidehpour, and Z. Schuss, "Effect of small random perturbations on power systems dynamics and its reliability evaluation," *IEEE Trans. Power Syst.*, vol. 4, no. 1, pp. 197–204, Feb. 1989.
[16] J. Qui, S. Shahidehpour, and Z. Schuss, "Random perturbation of transfer capability and its effect on power system reliability evaluation," *Int. J. Electr. Power Energy Syst.*, vol. 11, no. 4, pp. 253–266, Oct. 1989.
[17] K. Loparo and G. Blankenship, "A probabilistic mechanism for small disturbance instabilities in electric power systems," *IEEE Trans. Circuits Syst.*, vol. 32, no. 2, pp. 177–184, Feb. 1985.
[18] N. Forouzandehmehr, M. Esmalifalak, H. Mohsenian-Rad, and Z. Han, "Autonomous demand response using stochastic differential games," *IEEE Trans. Smart Grid*, vol. 6, no. 1, pp. 291–300, Jan. 2015.
[19] B. Yuan, M. Zhou, G. Li, and X. Zhang, "Stochastic small-signal stability of power systems with wind power generation," *IEEE Trans. Power Syst.*, vol. 30, no. 4, pp. 1680–1689, Jul. 2015.
[20] H. Mohammed and C. Nwankpa, "Stochastic analysis and simulation of grid-connected wind energy conversion system," *IEEE Trans. Energy Convers.*, vol. 15, no. 1, pp. 85–90, Mar. 2000.
[21] X. Wang, H. Chiang, J. Wang, H. Liu, and T. Wang, "Long-term stability analysis of power systems with wind power based on stochastic differential equations: Model development and foundations," *IEEE Trans. Sustain. Energy*, vol. 6, no. 4, pp. 1534–1542, Oct. 2015.
[22] D. Apostolopoulou, A. Dominguez-Garcia, and P. Sauer, "An assessment of the impact of uncertainty on automatic generation control systems," *IEEE Trans. Power Syst.*, vol. 31, no. 4, pp. 2657–2665, Jul. 2016.
[23] D. Podolsky and K. Turitsyn, "Random load fluctuations and collapse probability of a power system operating near codimension 1 saddle-node bifurcation," in *Proc. IEEE Power Energy Soc. General Meeting*, 2013, pp. 1–5.
[24] F. Milano and R. Zarate-Minano, "A systematic method to model power systems as stochastic differential algebraic equations," *IEEE Trans. Power Syst.*, vol. 28, no. 4, pp. 4537–4544, Nov. 2013.
[25] R. Zárate-Miñano, M. Anghel, and F. Milano, "Continuous wind speed models based on stochastic differential equations," *Appl. Energy*, vol. 104, pp. 42–49, Apr. 2013.
[26] Z. Dong, J. Zhao, and D. Hill, "Numerical simulation for stochastic transient stability assessment," *IEEE Trans. Power Syst.*, vol. 27, no. 4, pp. 1741–1749, Nov. 2012.
[27] M. Perninge, F. Lindskog, and L. Soder, "Importance sampling of injected powers for electric power system security analysis," *IEEE Trans. Power Syst.*, vol. 27, no. 1, pp. 3–11, Feb. 2012.
[28] T. Odun-Ayo and M. Crow, "Structure-preserved power system transient stability using stochastic energy functions," *IEEE Trans. Power Syst.*, vol. 27, no. 3, pp. 1450–1458, Aug. 2012.
[29] A. Kiani Bejestani and A. Annaswamy, "A dynamic mechanism for wholesale energy market: Stability and robustness," *IEEE Trans. Smart Grid*, vol. 5, no. 6, pp. 2877–2888, Nov. 2014.
[30] K. Wang and M. Crow, "The Fokker-Planck equation for power system stability probability density function evolution," *IEEE Trans. Power Syst.*, vol. 28, no. 3, pp. 2994–3001, Aug. 2013.
[31] C. De Marco and A. Bergen, "A security measure for random load disturbances in nonlinear power system models," *IEEE Trans. Circuits Syst.*, vol. 34, no. 12, pp. 1546–1557, Dec. 1987.
[32] W. Zhu, "Nonlinear stochastic dynamics and control in Hamiltonian formulation," *Appl. Mech. Rev.*, vol. 59, no. 4, pp. 230–248, 2006.
[33] H. Chang, C. Chu, and G. Cauley, "Direct stability analysis of electric power systems using energy functions: Theory, applications, and perspective," *Proc. IEEE*, vol. 83, no. 11, pp. 1497–1529, Nov. 1995.
[34] P. Kundur, N. Balu, and M. Lauby, *Power System Stability and Control,* 1st ed. New York, NY, USA: McGraw-Hill, 1994.
[35] X. Mao, *Stochastic Differential Equations and Their Applications,* 1st ed. Chichester, U.K.: Horwood, 1997.
[36] W. Zhu and Y. Yang, "Stochastic averaging of quasi-nonintegrable-hamiltonian systems," *J. Appl. Mech.*, vol. 64, no. 1, pp. 157–164, Mar. 1997.
[37] W. Zhu, Z. Huang, and Y. Yang, "Stochastic averaging of quasi-integrable hamiltonian systems," *J. Appl. Mech.*, vol. 64, no. 4, pp. 975–984, Dec. 1997.
[38] C. Gan and W. Zhu, "First-passage failure of quasi-non-integrable-Hamiltonian systems," *Int. J. Non-Linear Mech.*, vol. 36, no. 2, pp. 209–220, Mar. 2001.
[39] Y. Liu, T. Chen, C. Li, Y. Wang, and B. Chu, "Energy-Based L2 disturbance attenuation excitation control of differential algebraic power systems," *IEEE Trans. Circuits Syst. II: Express Briefs*, vol. 55, no. 10, pp. 1081–1085, Oct. 2008.
[40] Y. Sun, Y. Song, and X. Li, "Novel energy-based Lyapunov function for controlled power systems," *IEEE Power Eng. Rev.*, vol. 20, no. 5, pp. 55–57, May 2000.
[41] Y. Wang, D. Cheng, C. Li and Y. Ge, "Dissipative hamiltonian realization and energy-based L2-disturbance attenuation control of multimachine power systems," *IEEE Trans. Autom. Control*, vol. 48, no. 8, pp. 1428–1433, Aug. 2003.
[42] L. Cai, Z. He, and H. Hu, "A new load frequency control method of multi-area power system via the viewpoints of port-hamiltonian system and cascade system," *IEEE Trans. Power Syst.*, vol. 32, no. 3, pp. 1689–1700, May 2017.
[43] S. Dhople, Y. Chen, L. DeVille, and A. Dominguez-Garcia, "Analysis of power system dynamics subject to stochastic power injections," *IEEE Trans. Circuits Syst. I: Reg. Papers*, vol. 60, no. 12, pp. 3341–3353, Dec. 2013.
[44] G. Golub and C. Van Loan, *Matrix Computations*, 1st ed. Baltimore, MD, USA: The Johns Hopkins Univ. Press, 1996.
[45] D. Li, G. Ströhmer, and L. Wang, "Symmetry of integral equations on bounded domains," *Proc. Amer. Math. Soc.*, vol. 137, no. 11, pp. 3695–3695, Jun. 2009.

Ping Ju (M'95–SM'10) received the B.S. and M.S. degrees from Southeast University, Nanjing, China in 1982 and 1985, respectively, and the Ph.D. degree from Zhejiang University, Hangzhou, China, all in electrical engineering. From 1994 to 1995, he was an Alexander-von Humboldt Fellow with the University of Dortmund, Dortmund, Germany. He is currently a Professor of electrical engineering with Hohai University, Nanjing, China.

His research interests include modeling and control of power system, smart grid with renewable power generation.

Hongyu Li (S'14) received the B.S. degree in electrical engineering in 2012. He is currently working toward the Ph.D. degree in electrical engineering at Hohai University, Jiangsu, China. He is currently performing research at the University of Tennessee, Knoxville, TN, USA, as a visiting student.

His main research interest focuses on power system dynamic analysis under stochastic disturbances.

Chun Gan (S'14–M'16) received the B.S. and M.S. degrees in power electronics and motor drives from China University of Mining and Technology, Jiangsu, China, in 2009 and 2012, respectively, and the Ph.D. degree in power electronics and motor drives from Zhejiang University, Hangzhou, China, in 2016.

He is currently a Research Associate in the Department of Electrical Engineering and Computer Science, University of Tennessee, Knoxville, TN, USA. He has published more than 40 technical papers in leading journals and conference proceedings and authored one book chapter. He has ten issued/published invention patents. His research interests include high-efficiency power converters, electric vehicle, microgrid, electrical motor drives, and electrical motor design.

Dr. Gan received the 2015 Top Ten Excellent Scholar Award, the 2016 Excellent Ph.D. Graduate, the 2015 Ph.D. National Scholarship, the 2015 Wang Guosong Scholarship, and the 2014 and 2015 Outstanding Ph.D. Candidate in Zhejiang University.

Yong Liu (S'10–M'15) received the B.S. and M.S. degrees in electrical engineering from Shandong University, Jinan, China, in 2007 and 2010, respectively, and the Ph.D. degree from the University of Tennessee, Knoxville, TN, USA, in 2013.

He is currently a research assistant professor in the Department of Electrical Engineering and Computer Science, University of Tennessee. He is also a member of the DOE/NSF-cofunded engineering research center CURENT. His research interests include power system wide area measurement, renewable energy integration, and power system dynamic modeling and analysis.

Yiping Yu (M'10) received the B.Sc. and M.Sc. degrees in electrical engineering from Sichuan University, Chengdu, China, in 1999 and 2002, respectively, and the Ph.D. degree in electrical engineering from Tsinghua University, Beijing, China, in 2010.

He is an Associate Professor in the College of Energy and Electrical Engineering, Hohai University, Nanjing, China. From 2013 to 2014, he was also a visiting scholar at Georgia Institute of Technology. From 2002 to 2006, he was an EMS Engineer in China Electric Power Research Institute, Beijing, China. His research is on power system stability and control.

Yilu Liu (S'88–M'89–SM'99–F'04) received the B.S. degree from Xian Jiaotong University, Xi'an, China, and the M.S. and Ph.D. degrees from the Ohio State University, Columbus, OH, USA, in 1986 and 1989, respectively.

She was currently the Governor's Chair with the University of Tennessee, Knoxville, TN, USA, and Oak Ridge National Laboratory (ORNL). She was elected as the member of National Academy of Engineering in 2016. She is also the Deputy Director of the DOE/NSF co-funded engineering research center CURENT. Prior to joining UTK/ORNL, she was a Professor at Virginia Tech. She led the effort to create the North American power grid frequency monitoring network at Virginia Tech, which is now operated at UTK and ORNL as GridEye. Her current research interests include power system wide-area monitoring and control, large interconnection-level dynamic simulations, electromagnetic transient analysis, and power transformer modeling and diagnosis.